JOURNAL OF BALKAN GEOPHYSICAL SOCIETY, Vol.8, No 3, August 2005, p. 113-128

Accuracy evaluation of typical, infinite bandwidth, minimum time seismic modeling schemes

I. F. Louis, K. D. Marmarinos and F. I. Louis

Department of Geophysics and Geothermics, Faculty of Geology and GeoEnvironment, University of Athens, Panepistimiopolis, Ilissia, Athens 15784, Greece

Abstract: *The performance of a variety of travel time modelling schemes is evaluated, in terms of their accuracy, by using numerical simulations. The methods considered predict minimum travel times in two-dimensional P-wave velocity model parameterizations. They are typical, infinite bandwidth, seismic modeling schemes implemented in many inversion and imaging algorithms The methods considered include: the finite differencing approach of the eikonal equation as described by Vidale, the shortest path method as described by Moser and a variation of it as described by Nakanishi and Yamaguchi for calculation of seismic rays and first arrivals, and the two-point ray tracing technique as presented by Vesnaver. Quantitative comparisons between forward modeling approaches are based on the misfit between true and calculated travel times, number of model parameters used and the smoothness of the velocity field. When the constant velocity distribution is utilized Vidale's method is giving results within tolerance with respect to travel time accuracy in opposition to the ray perturbation and SPM scheme where the error is lower. For fine model parameterizations, Vidale's scheme remains the most efficient in computer time but still suffers in the error distribution. In stratified models, Vidale's scheme gives increasing errors for increasing velocity contrast. In smooth velocity fields a drop in the misfit is observed in the far field and the method is still computationally faster. Shortest path calculations are independent from the model whereas the error remains related to the number of possible routes. The two-point raytracing scheme performs better in smooth velocity fields giving time misfits strongly associated with the distance and smoothly decreasing for far offsets.*

Key words: *Forward Modelling, Travel Times Calculations, Vidale's Finite Differences Method, Shortest Path Method, Two-Point Ray Tracing Method.*

INTRODUCTION

Study of seismic wave propagation and excitation has been an important subject of seismology from the early times. It is the base of recovering the structure of the crust and upper mantle from the observed travel times of seismic waves, investigating the rupture nature of seismic sources, and exploring the structure and geophysical characteristics of the inner part of the Earth. Raypath tracing and travel time calculation are also essentials for a number of important near-surface imaging techniques such as tomographic calculation of statics from first arrivals. Traveltime calculation for these techniques differs from that for other applications in that, on land, velocities are usually most variable at shallow depths. As a result, an algorithm for near-surface traveltime calculation must be very robust and devoid of the shadow-zone problem which has greatly troubled the tomographic calculations based on traditional raytracing (e.g., Jackson and Tweeton, 1993). Moreover, as tomography is an iterative process and requires intensive ray tracing at each iteration, the algorithm must also be efficient in both traveltime and raypath calculation. A number of traveltime calculation techniques have been developed over the past decades which avoid the shadow-zone problem; the most widely used are perhaps the finite-

difference (e.g., Vidale, 1988, 1990) and wavefront construction (e.g., Vinje et al., 1993) methods. The wavefront construction methods are accurate in describing both traveltimes and raypaths, but require expensive global wavefront construction and traveltime interpolation from these wavefronts to grid points. In this research we demonstrate the accuracy and efficiency of the most typical, infinite bandwidth, schemes used to calculate the Fermat arrival of the wave equation using synthetic simulation examples.

TYPICAL, INFINITE BANDWIDTH, MINIMUM TIME MODELING SCHEMES

We have tested the suitability of three forward modeling schemes, belonging to the family of infinite frequency methods, to compute raypaths and traveltimes using synthetic models: the expanding computation fronts schemes, the graph theory methods, and the classic ray-theory methods. In recent years, following the extension of the random-access computer memory (RAM), many authors proposed several kinds of forward modeling solvers falling within the above categories.

Expanding computation front schemes – Vidale FAST2D propagator

Expanding computation front schemes are usually the fastest methods to compute travel times in heterogeneous media, although many implementations are not sufficiently accurate in regions with high velocity contrasts. In this study we have tested the method of Vidale (1988). Vidale proposed a finite difference scheme that involves progressively integrating the traveltimes along an expanding square. Strictly speaking, this method doesn't track wavefronts to determine the traveltime field, but represents a precursor to the class of schemes that do, and is still widely used. The velocity model is discretized to a grid of nodes with equal horizontal and vertical spacing. The basic idea is the numerical solution of the eikonal equation (1) in two dimensions that relates gradient of the traveltime (t) to the velocity structure:

$$\left(\frac{\partial t}{\partial x}\right)^2 + \left(\frac{\partial t}{\partial z}\right)^2 = S(x,z)^2 \qquad (1)$$

where x and z are the Cartesian coordinates and s is the slowness. Vidale's algorithm is using a calculation scheme of expanding square rings starting from the source location. The timing process is initiated by assigning source point the travel time zero. The travel times of the points adjacent to source are then calculated. Next the travel times for the four corners are found by solving numerically the eikonal equation. Each side of one of these rings is timed separately, moving from minimum to its neighboring maxima. The travel times are found throughout the grid by performing calculations on rings of increasing radius around the source point. The method is stable for smooth velocity models.

Graph theory methods - Shortest path ray tracing

The shortest path or network method uses Fermat's principle directly to find the path of the first-arrival ray between source and receiver. To achieve this, a grid of nodes is specified within the velocity medium and a network or graph is formed by connecting neighboring nodes with traveltime path segments. The first-arrival ray path between source and receiver will then correspond to the path through the network which has the least traveltime. Once the network structure and method of traveltime determination between two nodes has been chosen, the next step is to use a shortest path algorithm to locate the ray path. Essentially, the problem is to

locate the path of minimum traveltime from all the possible paths between source and receiver through the given network. An algorithm that is often used in network theory is that of Dijkstra (1959) for which computation time is proportional to the number of nodes squared.

Errors in SPR are due to the finite node spacing and angular distribution of node connectors (Moser, 1991). A coarse grid of nodes may poorly approximate the velocity variations while a limited range of angles between adjacent connectors may result in a poor approximation to the true path. Obviously, increasing the number of nodes and connectors will result in superior solutions but may come at a significant computational cost. Much work has been done to increase the computational speed of the shortest path algorithm, with particular attention given to the use of efficient sorting algorithms (Moser, 1991; Klime¡s and Kvasni¡cka, 1994; Cheng and House, 1996; Zhang and Toksöz, 1998).

In a seminal paper by Nakanishi and Yamaguchi (1986), the velocity field is defined by a set of constant velocity blocks with network nodes placed on the interface between the blocks. Connection paths between adjacent nodes do not cross any cell boundaries, so the traveltime t between two nodes is simply $t = ds$ where d is the distance between the two nodes and s is cell slowness. A similar approach is used by Fischerand and Lees (1993). Moser (1991) uses a rectangular grid with the network nodes coinciding with the velocity nodes. The traveltime between two connected nodes is estimated by $t = d(s_1 + s_2)/2$ where s_1 and s_2 are the slowness at the two nodes.

The number of points considered to be neighbors (described from Moser as forward star) varies. In this study, 2nd and 3rd order graph templates (Fig. 1) are used.

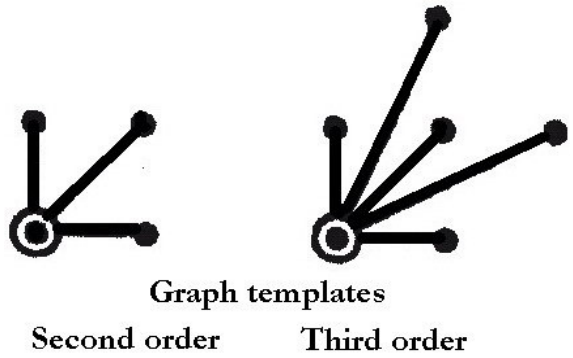

FIG. 1. Second and third order graph templates (Matarese, 1993).

Classic ray theory methods - Two-point ray tracing schemes

The two-point raytracing scheme developed by Vesnaver (1993) is examined. It is a minimum time two point ray tracer, operating on irregular grids, based on the Fermat's principle of minimum time. It simulates all types of waves, including reflected, refracted, diffracted and converted waves. An optimized version of this algorithm modified for parallel computing in a distributed heterogeneous environment is also used (Kofakis and Louis, 1994).

In this method the ray tracing algorithm starts using an initial guess for the ray path that connects the source and the receiver points. In homogeneous media, the ray is a straight line with fixed end points opposed to heterogeneous media where the bending of the ray is an iterative search for the minimum time

path that satisfies Fermat's principle. Since the minimum travel time path is a summation of minimum travel time segments, the minimum time condition is applied also in the straight-line segments inside each velocity pixel. The intersection point of each ray with the pixel side (2-D case) is perturbed along the side in a way that ensures the minimum time condition (Böhm et al., 1999). An usual approach in this case is, among the neighbor pixels, to choose the ray with the highest velocity. The minimization through iterations of the initial guess is the minimum time ray path.

Whereas analytical methods fail to compute the response of complex synthetic models, other methods, based on the solution of the full-wave equation, have been proposed in the past to solve the problem. ACO2D (Vafidis, 1992) is a finite difference vectorized propagator with a second order in time and fourth order in space accuracy, describing acoustic wave propagation in a two dimensional heterogeneous medium. In order to calculate the earth response the equivalent first-order hyperbolic system of equations given below is solved numerically. This system consists of the basic equations of motion in the x and z directions, namely:

$$\rho(x,z)\frac{\partial}{\partial t}\dot{u}(x,z,t)=\frac{\partial}{\partial x}p(x,z,t) \quad (2)$$

$$\rho(x,z)\frac{\partial}{\partial t}\dot{w}(x,z,t)=\frac{\partial}{\partial z}p(x,z,t) \quad (3)$$

and the pressure-strain relation after taking the first time derivatives:

$$\frac{\partial}{\partial t}p(x,z,t)=K(x,z)[\frac{\partial}{\partial z}\dot{w}(x,z,t)+\frac{\partial}{\partial x}\dot{u}(x,z,t)] \quad (4)$$

where the time derivatives of $u(x,z,t)$ and $w(x,z,t)$ represent the vertical and horizontal components of the particular, the first arrival travel times particle velocity, respectively, $p(x,z,t)$ denotes the pressure field, $\rho(x,z,)$ is the density of the medium and $K(x,z)$ is the bulk modulus. Equations (2)-(4) can be written in matrix form as

$$\frac{\partial}{\partial t}\begin{bmatrix}p\\ \dot{u}\\ \dot{w}\end{bmatrix}=\begin{bmatrix}0 & K & 0\\ 1/\rho & 0 & 0\\ 0 & 0 & 0\end{bmatrix}\frac{\partial}{\partial x}\begin{bmatrix}p\\ \dot{u}\\ \dot{w}\end{bmatrix}+\begin{bmatrix}0 & 0 & K\\ 0 & 0 & 0\\ 1/\rho & 0 & 0\end{bmatrix}\frac{\partial}{\partial z}\begin{bmatrix}p\\ \dot{u}\\ \dot{w}\end{bmatrix}$$

or

$$\frac{\partial}{\partial t}U=A\frac{\partial}{\partial x}U+B\frac{\partial}{\partial z}U$$

which is a first-order hyperbolic system.

Dispersion analysis indicates that the shortest wavelength in the model needs to be sampled at six grid points/wavelength and the stability criterion is governed by $\Delta t<2/3(\Delta x/V_{\max})$, where $V_{\max}$ is the maximum wave velocity, Δt is the time step and Δx is the grid digitization interval. A spatially localized source is implemented by specifying the initial conditions applied to both particle velocity and pressure and using the source insertion principle of Alterman and Karal (1968). A buried line source is inserted having a Gaussian time excitation function.

ACO2D propagator was implemented as the reference algorithm to compute the travel time residuals, and consequently the accuracy of the evaluated schemes.

TRAVELTIME MODELING EVALUATION

The selection of the numerical method to calculate travel times depends on the nature of the travel times, on the complexity of the seismic model of the geologic structure, on the geometry of the set of nodes at which the travel times is to be calculated and on the accuracy required. When selecting the travel-time calculation method, we should consider the kind of travel-times to calculate. In (often but not always required in seismic

travel-time tomography) were adopted. On the other hand, seismic model of the medium is, as a rule, specified by a finite set of values (model parameters), and of the rules or procedures expressing the dependence of spatial variations of material properties on these values. Since the exact material properties are fractal in the nature, the material properties described by the model are, as a rule, smoothed approximations of the exact ones. Thus the smoothness is a natural property of a seismic model. Moreover, probably all cotemporary numerical methods of wavefield or travel-time calculation requires in some sense smooth models.

When simple geometric models are considered the accuracy of the method examined is determined by comparing the computed travel-times with those obtained by solving the forward modeling problem with analytical methods. For complex synthetic models, where the analytical methods fail to solve the problem, synthetic travel-times computed with very accurate methods based on the solution of the full- wave equation are used to test the accuracy of the method examined.

The residuals $t - t'$, between the computed travel times t' and those obtained by analytical methods or by solutions of the full-wave equation methods t, are demonstrated by the absolute relative per cent error given by:

$$\sigma = \left| \frac{t - t'}{t} \right| \cdot 100\%$$

Three different synthetic velocity models were used to evaluate the accuracy of the forward modeling methods examined: the simple homogeneous model, a simple stratigraphic model with horizontal interfaces and layers with constant velocities, and a complex velocity model demonstrating real geologic structures with dipping layers, faults and lateral velocity variations.

Homogeneous Model

A homogeneous velocity model (Fig. 2) with a constant velocity of 1500 m/s is used for the numerical simulations. It has dimensions 110 x 110 m and a single seismic source is located in the center of the medium.

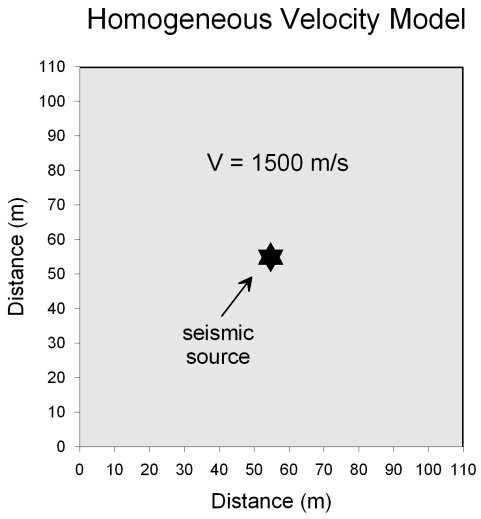

FIG. 2. Homogeneous model.

Vidale's FAST2D propagator was first implemented to compute the travel time response of the model. Three different model discretization schemes were implemented (grids of 15x15, 30x30 and 65x65 nodes) to compute the response. Figure 3 shows the distribution of the travel time propagation error for different grids of nodes.

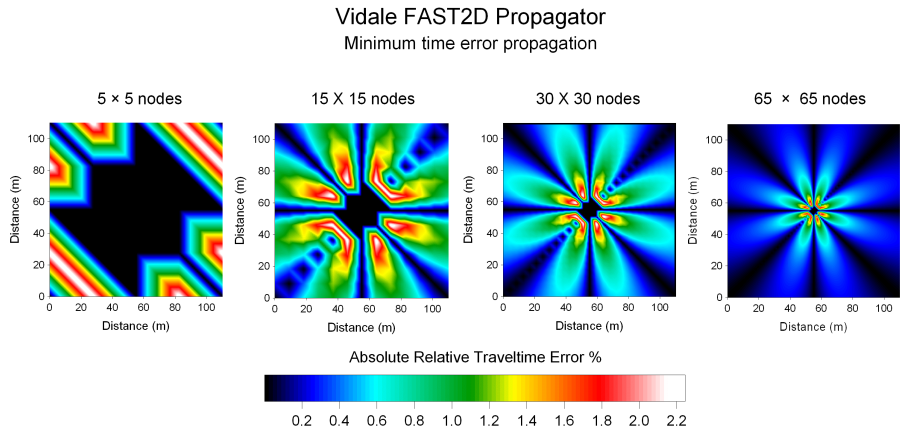

FIG. 3. Distribution of the travel time propagation error.

Large travel time misfits (residuals) and relative travel time errors are observed in the neighborhood of the source (Fig. 3) because of the poor approximations of the finite difference scheme to the eikonal equation in the vicinity of the source. With increasing radius, the wavefronts are become more planar, the approximations are more accurate and the relative errors drop quickly to zero. The performance of FAST2D propagator is improved when the grid of nodes of the discretized model increases.

In applying the two-point raytracing method, three different model discretization schemes were implemented (grids of 4x4, 8x8 and 16x16 cells) to compute the first arrival times. For comparison reasons, similar grids of nodes, like those used in the evaluation of Vidale's FAST2D propagator, were superimposed on the model. The nodes were considered as the edge points (geophones) of two-point raypaths, where the start point denotes the source position. The MINT2D raytracer developed by Vesnaver (1993) was implemented to compute the travel time response of the model. For case of a 16x16 cells model discretization, Figure 4 illustrates the distribution of the travel time propagation error for different grids of nodes. Like with FAST2D propagator, we observe here a similar character in the propagation of error by an accumulation of errors in the near-source region and gradually decreasing in the far field. From the same figure it is also evident that the performance of MINT2D raytracer is improved when the grid of cells of the discretized model increases. A comparison of Figures 3 and 4 shows that MINT2D raytracer achieves less accuracy compared to FAST2D finite difference propagator.

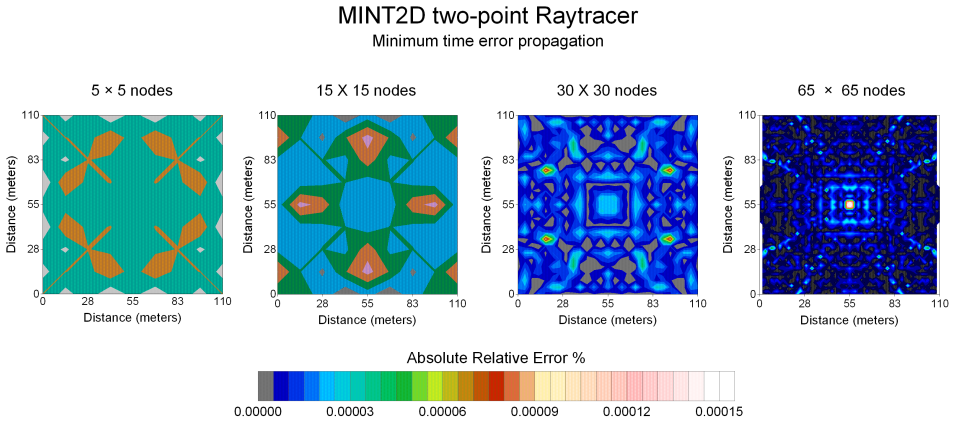

FIG. 4. Distribution of the travel time propagation error.

Unlike previous schemes, graph theory method, applied in second and third order graph templates, exhibits accuracy that is independent of radius. Moser's SPM raytracer was implemented to compute the travel time response of the model for a different number of grid nodes. The template used in this algorithm computes travel-times exactly along certain propagation directions. In all other directions, the traveltime errors accumulate at a constant rate, which implies that the percent error is a function of angle only. The upper part of Figure 5 shows the error propagation when a second order graph template is implemented. By employing more accurate graph templates (see lower part of Figure 5) we obtain improved results.

In employing Nakanishi-Yamaguchi version of Moser's SPM method, the velocity model is discretized in square cells where the nodes determining the ray path lay on the cells sides. Testing the method appears to be a little bit more complicated since, due to the grid complexity, more parameters are necessary to determine the optimum number of velocity cells and grid of nodes per cell's side. Figure 6 illustrates the propagation of error for various cell discretizations keeping a constant load of nodes (9X9).

Moser's method and its version presented by Nakanishi and Yamaguchi seem to offer the better accuracy of the methods examined.

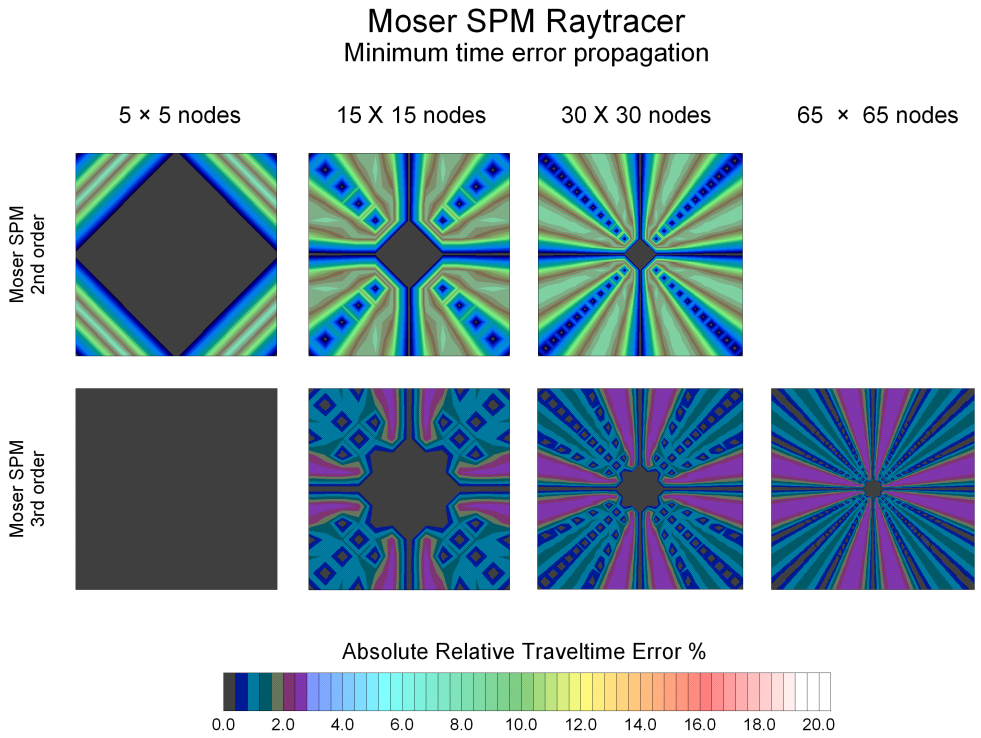

FIG. 5. Distribution of the travel time propagation error.

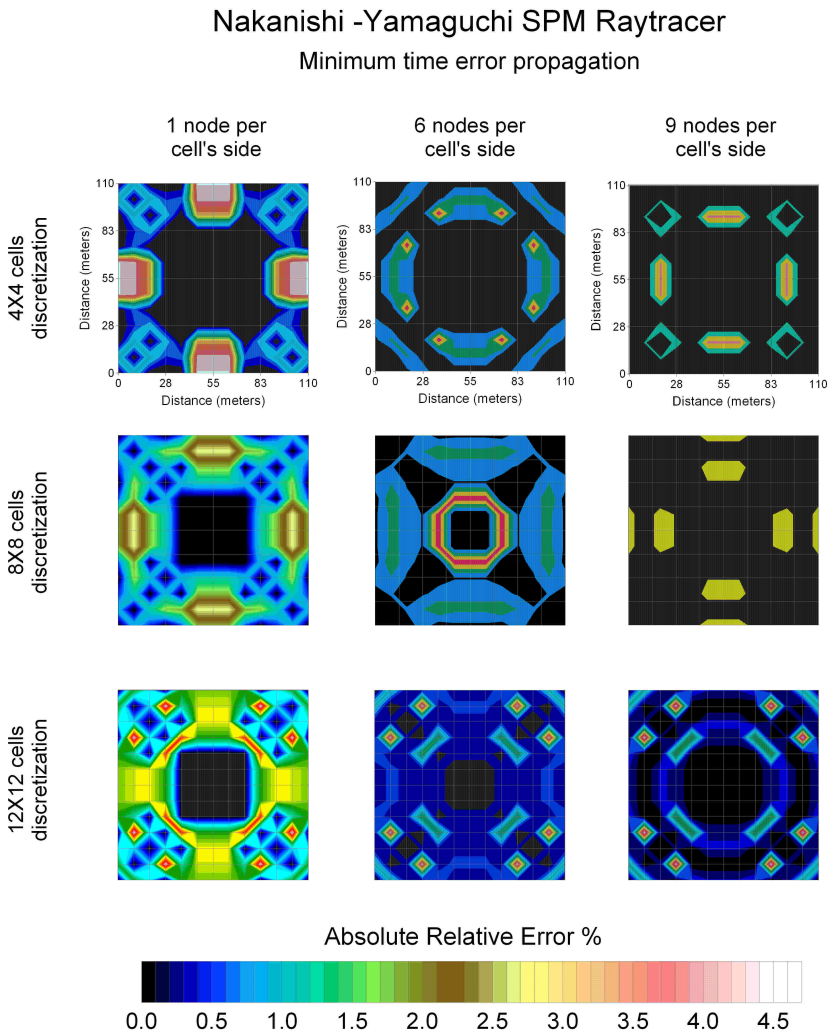

FIG. 6. Distribution of the travel time propagation error.

The Layered Model

A stratified velocity model provides a yet more practical modeling example and we choose here survey geometry typical of ground surface experiments. Figure 7 shows the velocity structure with a source situated in the upper left corner of the model which is composed of two layers with a horizontal interface is examined. It has dimensions 100x100 meters and the thickness of the surface layer is 10 m. The velocity of the surface layer is set to 1000 m/s, while two velocity values were implemented for the substratum: a velocity of 1100 m/s to denote the case of the smooth velocity model and velocities of 1600 and/or 2100 m/s for the case of high velocity contrasts.

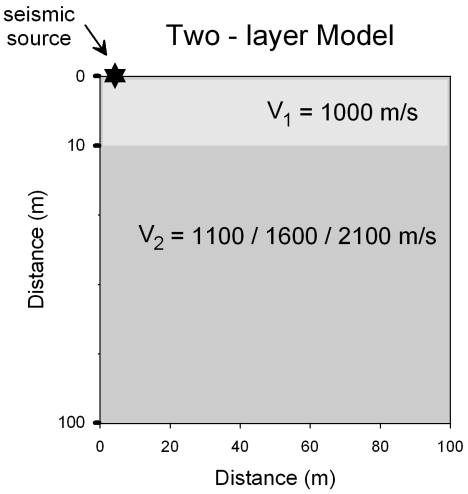

FIG. 7. The layered model.

A constant load of 30x30 grids of nodes was implemented to compute the response and accuracy of the methods

examined. The classic formulas $t = x/V_1$ and $t = \frac{x}{V_2} + 2h\frac{\sqrt{V_2^2 - V_1^2}}{V_1 \cdot V_2}$ were used for the analytical computation of the minimum travel times, where t is the travel time, x is the horizontal Euclidean distance between a point and the source, h is the upper layer thickness and V_1, V_2 are the velocities of the layers. Comparisons were performed only for the minimum times recorded at nodes (geophones) on the model surface.

Figure 8a illustrates the graph of the minimum time propagation error versus distance from the source when applying Vidale's Finite Difference propagator FAST2D. From the graph it is evident that the minimum time error remains stably low (<1%) for models with low velocity contrasts. For higher contrasts an abrupt increase of the error is observed in the neighborhood of the source because of the poor finite difference approximations to the eikonal equation in this area. This discrepancy arises from the inability of the eikonal methods to deal with sharp velocity contrasts, since these discontinuities violate the assumptions of the eikonal equation. With increasing radius, the approximations are more accurate and the relative errors drop quickly to zero.

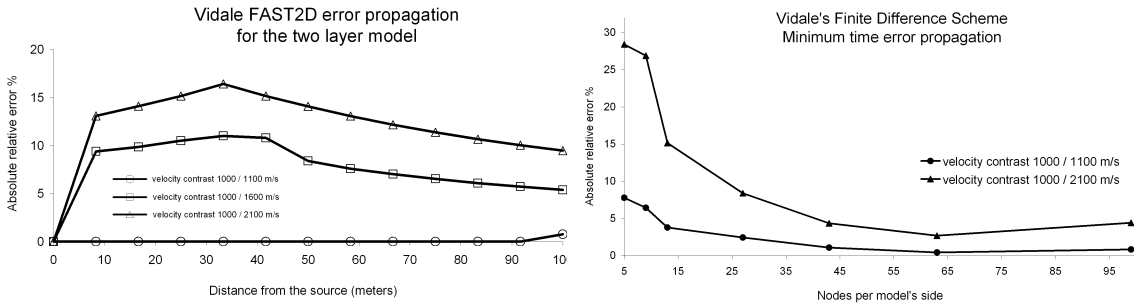

(a) **(b)**

FIG. 8. Travel time propagation error versus distance from the source (a) and number of discretization nodes.

Figure 8b illustrates the absolute relative percent error versus number of discretization nodes. From the same figure it is also evident that the performance of FAST2D propagator is improved when the grid of nodes increases. Higher error values, following however a similar performance, are also observed for higher velocity contrasts raised from the inability of the eikonal methods to deal with sharp velocity contrasts, since these discontinuities violate the assumptions of the eikonal equation.

In applying the MINT2D two-point raytracer, model requires the definition of the refraction interface. Since, for this method, the model discretization in cells stands only for the horizontal dimension, a series of 2, 10, 50 and 100 cells were examined. For comparison reasons again, a grid of 30x30 nodes like it used for the evaluation of Vidale's Finite Difference scheme was superimposed on the model. The nodes were considered again to represent the edge points (geophones) of two-point raypaths, where the start point denotes the source position. Similarly, comparisons were made only for the minimum times recorded at nodes (geophones) on the model surface.

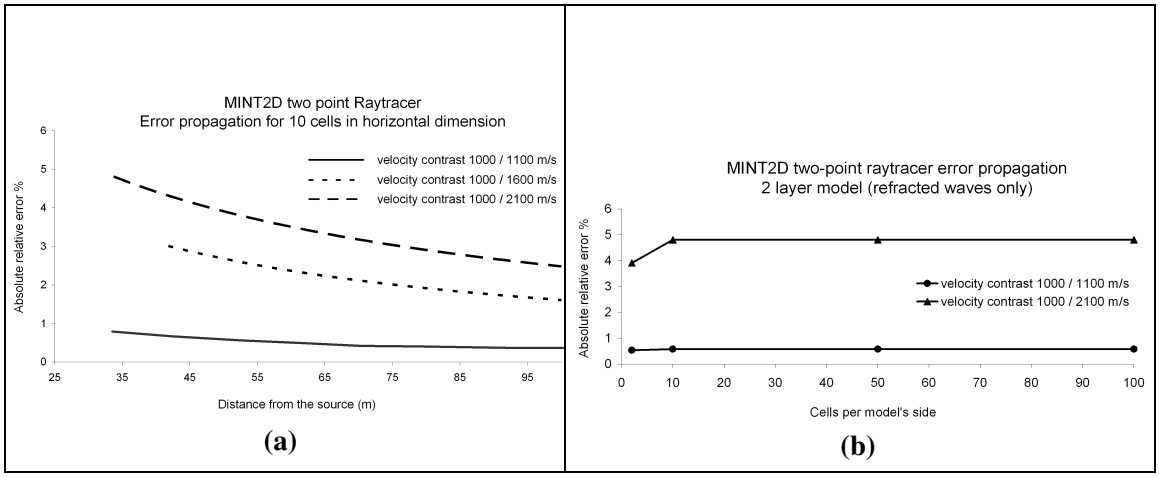

FIG. 9. Travel time propagation error versus distance from the source (a) and number of discretization cells.

The graph of the minimum time error propagation versus distance from the source is shown in Figure 9a. It is evident from the graph that, for low velocity contrasts (smooth fields), minimum time error remains low (<1%) descending smoothly towards the far offsets. With increasing velocity contrasts, higher error values are observed following similarly the same descending behavior. Figure 9b shows the minimum time error behavior versus the number of the discretization cells. It is evident from the figure that it generally keeps stably low values (<1%). Especially, a slight increase is observed up to the number of 50 discretization cells while it remains stable for higher discretization schemes.

Figure 10 shows the plot of the minimum travel time error propagation versus distance from the source for Moser's SPM raytracer using second order templates. Figure 11 shows the minimum travel time propagation error versus the number of discretization nodes per model's side.

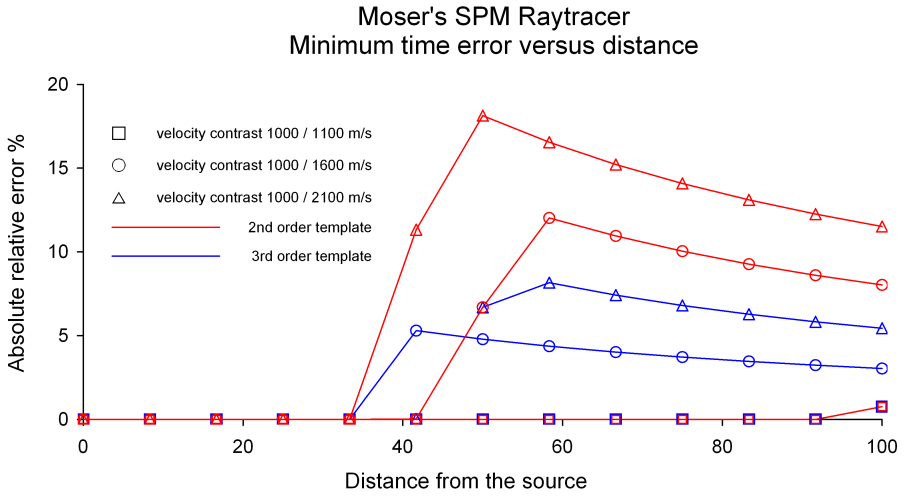

FIG. 10. Travel time propagation error versus distance from the source.

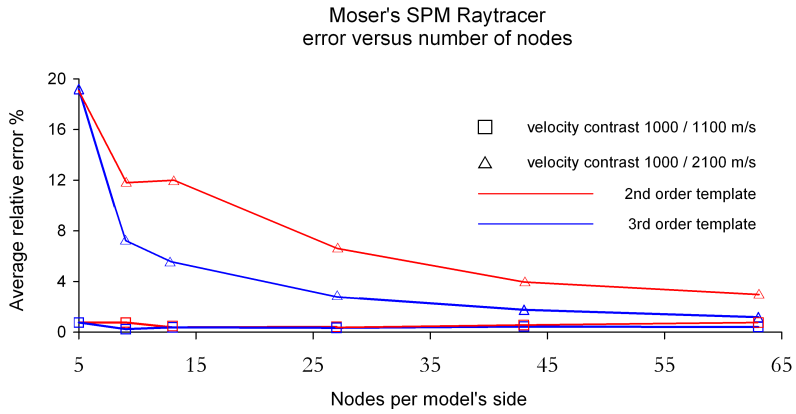

FIG. 11. Travel time propagation error versus number of discretization nodes.

From the interpretation of the error versus distance graphs it is evident that the minimum time error remains stably low (<1%) for the smoothly varying model. For higher velocity contrasts, abrupt changes in the minimum time errors are observed around the respective critical distances of 34 and 42m from the source, giving maximum respective error values of 12 and 18%. Beyond critical distance, the error is descending asymptotically towards the far offsets. Matarese (1993) explains the error jumps as the graph theoretical approach fares somewhat poorly in modeling Fermat times across jumps in the velocity field, due to the nature of its extrapolation template. Since the template only allows propagation in certain directions, it does not accurately predict excitation of the head wave. Consequently, this error propagates to all first arrivals associated with the head wave. Similar error behaviors are also observed by using third order templates (Figs. 10 and 11).

Nakanishi - Yamaguchi SPM raytracer

Figure 12 illustrates the minimum time error propagation versus distance from the source computed by incorporating the SPM raytracer, developed by Nakanishi and Yamaguchi. The travel times for 100 sampling points in the model's surface were compared with the analytical solution and the absolute relative error was calculated. The velocity contrasts are shown in the legend. Abrupt error changes are observed in the near source area following a descending pattern (<3%) in far offsets.

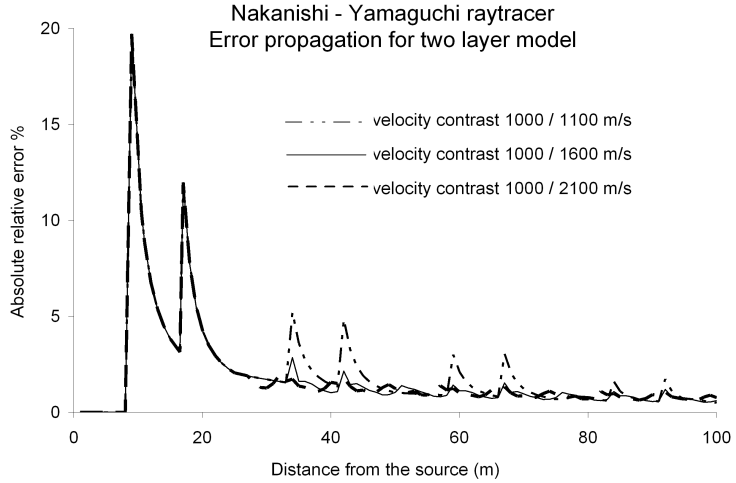

FIG. 12. Travel time propagation error versus distance from the source.

Another useful tool to understand the behavior of error is the diagrams of Figure 13, where the absolute relative minimum time error is plotted versus the number of discretization cells and the number of nodes per cell's side. The arrows show the error's reduction. From the direction and the size of these arrows one can observe that the error is decreasing intensively while the number of nodes is increasing and also the decreasing rate is higher for smaller nodes number.

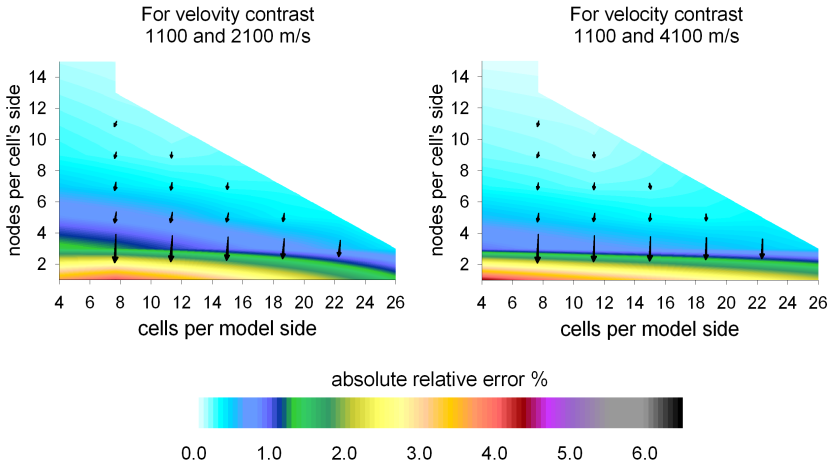

FIG. 13. Travel time error versus number of discretization cells and nodes per cell's side.

As far as the number of cells-error relationship is concerned, the error appears to be decreasing slowly, or even to be increasing in some cases, while more velocity cells are used. Nakanishi-Yamaguchi method reduces the error below 2 % when at least 3 nodes are used per cell's side and below 0.5 % when 9 nodes are used. Nakanishi and Yamaguchi version of Moser's graph theory method seems to offer the lowest error values compared with those observed by the rest of methods examined.

The Salt Model

The salt model represents a complex structure with irregular interface geometry (Fig. 14) and constant velocity blocks. It is 1000 m long and 500 m deep with a seismic source located at the grid point (100, 5). A string of 32 geophones at 20 m intervals is placed at a depth of 5 m with the first geophone at 300 m from the origin of the model.

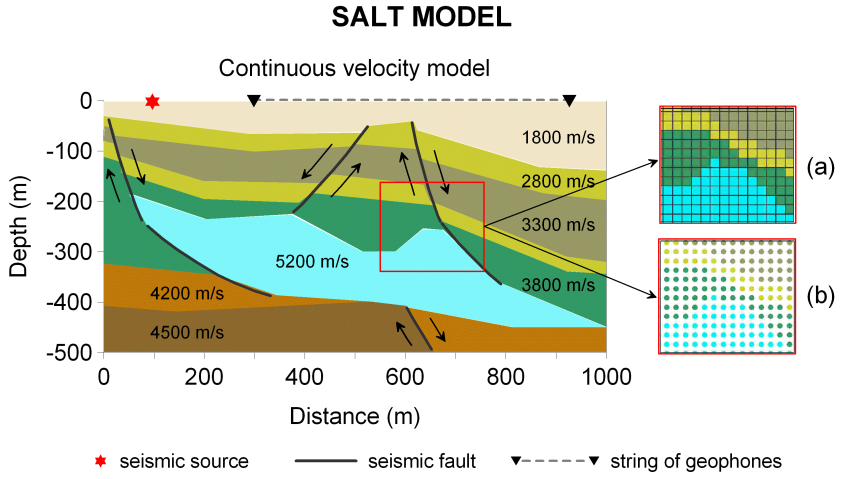

FIG. 14. The salt model.

Since analytical methods fail to compute the true theoretical response of the model, ACO2D finite difference propagator was implemented as a more accurate method to achieve it. To fulfill the demands of the methods examined, salt model was discretized both in cells and grid of nodes (Figs. 14a and b). Ray and wave fields (Figs. 15a and b) were produced and minimum travel time versus distance curves were obtained for their evaluation.

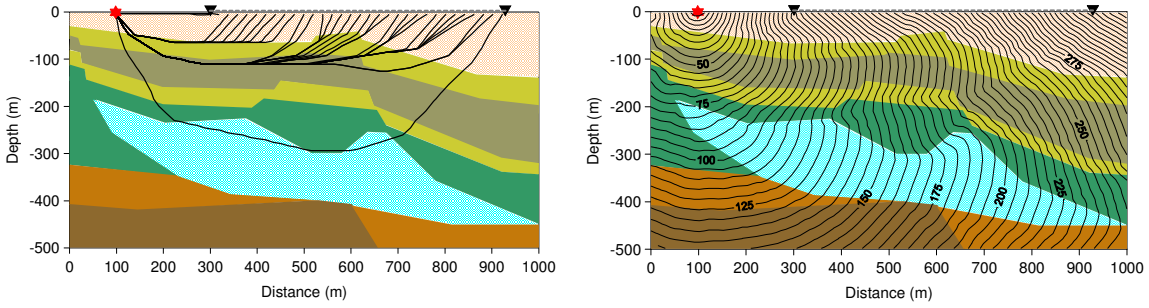

(a) **(b)**

FIG. 15. Ray and wave fields of the model.

Figure 16 shows the travel time plots of the evaluated modeling schemes as a function of distance from the source. For comparison reasons, the theoretical response of the model, achieved by implementation of ACO2D full-wave propagator, is also included in the graph.

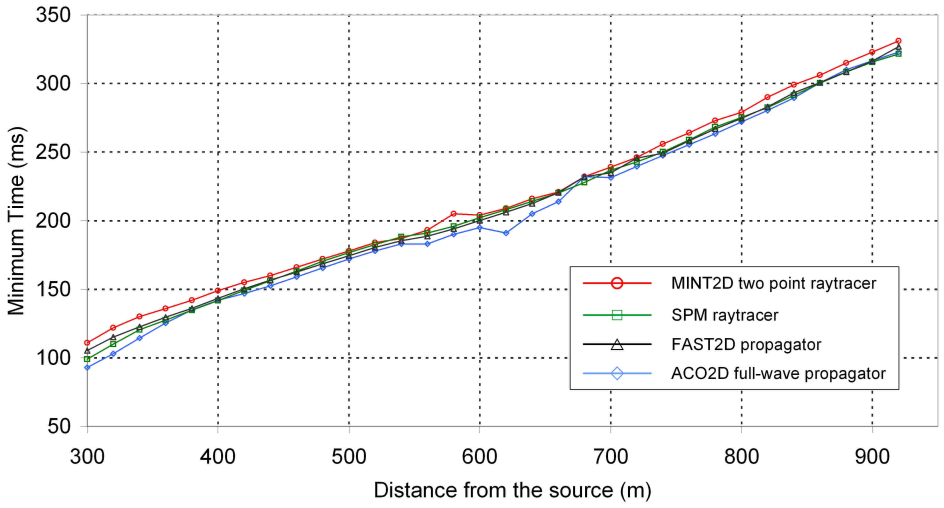

FIG. 16. Travel time plots for the different modeling schemes.

Figure 17 illustrates the minimum travel time propagation error as a function of distance from the seismic source computed by incorporating all the methods examined. It is evident from the figure that abrupt error changes are observed in the near source area following by a descending pattern (<3%) in the far offsets. Nakanishi – Yamaguchi version of shortest path method reduces the error below 1% in middle and less than 0.5% in the far offsets when 5 nodes are used per cell's side. Like the case of stratigraphic model, Nakanishi – Yamaguchi method seems to offer the lowest error values for the salt model.

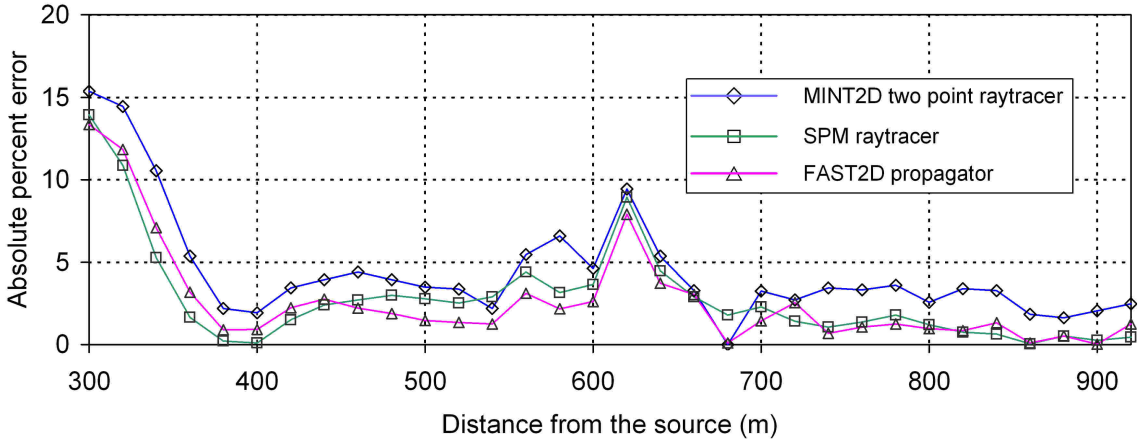

FIG. 17. Travel time error versus distance from the source for the different modeling schemes examined.

CPU Times

CPU times taken as a function of cell size (number of cells) or grid mesh size (number of grid nodes) were also estimated for the case of salt model. Calculations were performed with an ordinary personal computer with a single CPU (2.5 GHz), 1024 MB memory space and Windows XP operating system. Figures 18a to 18c show the estimated CPU times as a function of cell or grid mesh size for the methods examined. It is clear from the graphs that FAST2D finite difference propagator is significantly faster. SPM raytracer is the slowest method.

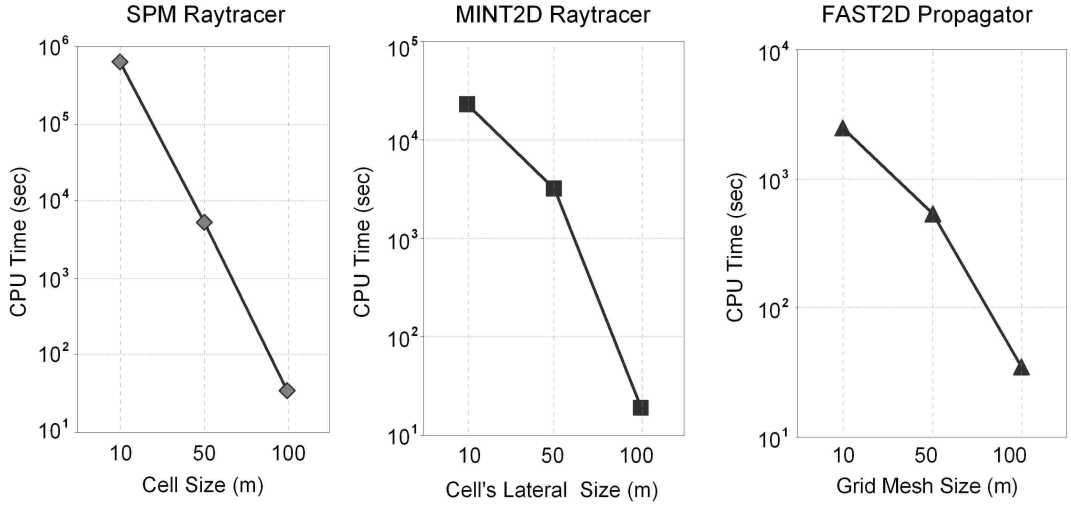

(a) (b) (c)

FIG. 18. CPU times.

CONCLUSIONS

Of the three approaches for travel time modeling discussed here, FAST2D propagator is an easy to use and relatively fast algorithm calculating first arrival times. It models only the kinematical properties of the wave equation and it works satisfactory in complex models with smooth velocity contrasts. Its sequential scheme makes it not easily converted to parallel implementation.

MINT2D two point ray-tracer works very satisfactory in relatively complex models and travel times for later

seismic arrivals are also calculated. It has a strong parallel decomposition aspect making it ideal for parallel implementation.

SPM raytracer is the slowest method but it computes raypaths as well as traveltimes. There are not restrictions of classical ray theory; diffracted raypaths and paths to shadow zones are found correctly. There are no problems with convergence of trial raypaths toward a specified receiver or with raypaths with only a local minimal traveltime. Unlike the other methods, SPM raytracer exhibits accuracy that is independent of distance. The template used in this algorithm calculates traveltimes exactly along certain propagation directions. In all other directions, the traveltime residual accumulates at a constant rate; thus the per cent error is a function of angle only.

ACO2D algorithm is full waveform finite-difference propagator. It models the kinematical and dynamic properties of the seismic waves and produces synthetic seismograms, which can be extremely useful in the interpretation procedure, when compared with the actual field seismograms. Its structure is ideal for implementation on vector computers.

ACKNOWLEDGEMENTS

The present study was funded through the program EPEAEK II in the framework of the project "PYTHAGORAS II, Support of University research groups" with contract number 70/3/8023.

REFERENCES

Böhm, G., Rosssi, G., Vesnaver, A., 1999, Minimum time ray-tracing for 3-D irregular grids: Journal of seismic exploration, **8**, 117-131.

Constable, S. C., Parker, R. L., Constable. C. G, 1987, Occam's inversion: A practical algorithm for generating smooth models from electromagnetic sounding data: Geophysics, **52**, 289–300.

Dellinger, J., 1991, Anisotropic finite-difference traveltimes: 61st Annual Internat. Mtg., Soc. Expl. Geophys., Expanded Abstracts, p. 1530-1533.

Dijkstra, E. W., 1959, A note on two problems in connection with graphs: Numer. Math., **1**, 269–271.

Fischer, R., and Lees, J. M., 1993, Shortest path ray tracing with sparse graphs: Geophysics, **58**, 987-996.

Gallo, G., Pallottino, S., 1986, Shortest path methods: A unifying approach: Mathematical Programming Study, **26**, 38-64.

Indira N. K. and Gupta P. K., 1998, Inverse methods: Narosa publishing house, p.1-53.

Jackson, D.D., 1972, Interpretation of inaccurate, insufficient, and inconsistent data: Geophys. J. Roy. Astr. Soc, **28**, 97-17.

Johnson, D. B., 1977, Efficient algorithms for shortest paths in sparse networks: Journal of the ACM, **24**, 1-13.

Klimeŝ M. and Kvasniĉka M., 1994, Three dimensional network ray tracing: Geoph. J. Int., **116**, 726-738.

Kofakis, G. P. and Louis, F.I., 1995, Distributed parallel implementation of seismic algorithms. In Mathematical Methods in Geophysical Imaging III, Siamak Hassanzadeh, Editor, Proc. SPIE 2571, 229-238, San Diego, California.

Liu, Q., 1991, Solution of the tree dimensional eikonal equation by an expanding wavefront method: 61st Annual Internat. Mtg., Soc. Expl. Geophys., Expanded Abstracts, p. 1488-1491.

Matarese, J. R., 1993, Nonlinear traveltime tomography: PHD thesis submitted at the Massachusetts

Institute of Technology (M.I.T.), department of Earth, Atmospheric and planetary Sciences.

McGaughey, W.J. and Young, R.P., 1990, Comparison of ART, SIRT, Least-Squares, and SVD Two-Dimensional Tomographic Inversions of Field Data. 60th Annual International Meeting of Society of Exploration Geophysicist, Expanded Abstracts, pp. 74-77.

Meju, M., 1994, Geophysical data analysis: Understanding inverse problem theory and practice: Society of Exploration Geophysicists, Course notes series, vol. 6.

Moser, T. J., 1991, Shortest path calculation of seismic rays: Geophysics, **56**, 59–67.

Nakanishi, I., Yamaguchi, K., 1986, A numerical experiment on nonlinear image reconstruction from first arrival times for two-dimensional island arc structure: J. Phys. Earth, **34**, 195-201.

Papazachos, C. and Nolet, G., 1997, Non-linear arrival tomography: Annali di geophysica, **40**, N. 1.

Qin, F., Luo, Y., Olsen, K. B., Cai, W., Schuster, G. T., 1992, Finite-difference solution of the eikonal equation along expanding wavefronts: Geophysics, 57, no. 3, p. 478–487.

Redpath, B. B., 1973, Seismic refraction explosion for engineering site investigations, Explosive excavation research laboratory, Livermore, California. Distributed by NTIS, p 5-7.

Schneider, W. A. Jr., Ranzinger, K. A., Balch, A. H., Kruse, C., 1992, A dynamic programming approach to first arrival traveltime computation in media with arbitrary distributed velocities: Geophysics, **57**, 39-50.

Tikhonov, A. N., 1963, Regularization of ill-posted problems. Doklay Akad. Nauk. SSSR, 153, p. 1-6.

Tikhonov, A. N., Arsenin, V. Y., 1977, Solution of ill-posted problems, John Wiley and Sons. Inc.

Tikhonov, A. N., Glasko, V. B., 1965, Application of a regularization method to nonlinear problems: J. Comp. Math. and Math. Phys, **5**, no.3.

Twomey, S., 1963, On the numerical solution of Freedom integral equations of the first kind by the inversion of the linear system produced by quadrature: J. Assn. Comput. Mach., **10**, 97-101.

Van Trier, J., and Symes, W. W., 1991, Upwind finite-difference calculation of traveltimes: Geophysics, **56**, 812–821.

Vesnaver, A., 1996, Ray tracing based on Fermat's principle in irregular grids: Geophysical Prospecting, **44**, 741-760.

Vidale, J., 1988, Finite-difference calculation of travel times: Bull. Seism. Soc. Am., **78**, 2062–2076.

Wattrus, N. J., 1991, Three dimensional finite-difference traveltimes in complex media: 61st Annual Internat. Mtg., Soc. Expl. Geophys., Expanded Abstracts, p. 1106-1109.

Weber, Z., 1995, Some improvement of the shortest path ray tracing algorithm. In: Diachok, O., Caity, A., Gerstof P., Schmidt, H. (Eds), Full Field Inversion Methods in Ocean and Seismo-Acoustics. Kluwer Academic Publishers, Dordrecht, 51-54.

Zhang, J., Toksöz, M. N., 1998, Nonlinear refraction travel time tomography: Geophysics, **63**, 1726-1733.